Synergistic effects of electrical and optical excitations on TiO_2 resistive device*

Qi Mao(毛奇)[1,2,†], Wei-Jian Lin(林伟坚)[1], Ke-Jian Zhu(朱科建)[1], Yang Meng(孟洋)[1,2], and Hong-Wu Zhao(赵宏武)[1,2,‡]

[1] *Beijing National Laboratory for Condensed Matter Physics, Institute of Physics, Chinese Academy of Sciences, Beijing* 100190, *China*
[2] *School of Physical Sciences, University of Chinese Academy of Sciences, Beijing* 100049, *China*

(Received 24 March 2017; revised manuscript received 18 April 2017; published online 20 June 2017)

The influences of electrical and optical excitations on the conductivity characteristic are investigated in bulk and edge devices of ITO/TiO_2/ITO structure. Driven by the electrical and optical stimuli independently, the conductivity relaxation behaviors of the pristine resistive state (PRS) are observed and ascribed to the electron trapping and the oxygen transport processes. For a resistive switching (RS) device, the conductance change under optical illumination is about two orders of magnitude smaller than the conductance change corresponding to the variation of background current due to the emergence of a great number of oxygen vacancies in the RS device. With the illumination being off, the conductance slowly decays, which suggests that the oxygen diffusion process dominates the conductance relaxation. The difference in conductance relaxation between the bulk and edge devices indicates that the oxygen exchange plays a critical role in the relaxation process of conductivity. The synergistic effects of both electrical and optical excitations on the RS devices could be used for novel applications in integrated optoelectronic memory devices.

Keywords: resistance switching, photoconductance, relaxation, oxygen vacancy

PACS: 77.80.Fm, 72.40.+w, 68.55.Ln, 73.50.Gr **DOI:** 10.1088/1674-1056/26/8/087702

1. Introduction

When subjected to an electric field, metal oxide films sandwiched between electrodes may exhibit the resistive switching (RS) effect, which describes a reversibly resistance change between a high resistance state (HRS) and a low resistance state (LRS).[1–4] The RS behaviors in oxides have drawn a great deal of attention for their potential applications in future nonvolatile memory devices. Accordingly, the migration and diffusion of oxygen vacancies driven by the electric field have been proposed to play a critical role in the RS process of oxide films.[5–10] Meanwhile, some metal–oxide semiconductors, such as TiO_2, ZnO, and WO_3, manifest large change of conductivity under optical irradiation.[11–14] These photoconductivity characteristics have provided useful information about the oxygen vacancies in the oxide from another perspective, such as distribution of sub-bandgap states,[11,13] surface states, and adsorption.[12,14] Recently, it has been reported that the RS properties of oxides can be dramatically modulated by optical illumination by realizing optical writing and multilevel storage in the memory devices.[15–20] Several models have been suggested to explain the optically modulated RS phenomena, including electron trapping/detrapping,[18] carrier injection,[15,19,20] and chemical adsorption/desorption molecules on the surface.[16,17] However, the mechanism of the optically induced modification of the RS is still a matter of debate, due to the fact that the optically induced conductivity change during the RS is actually an emergent property resulting from the synergy effect of oxygen vacancies under optical and electrical stimulation. Therefore, a better understanding of the optically modulated RS should be based on systematic investigations of the conductance change driven independently by the electrical and optical stimuli and their interplay.

In this paper, we report the influences of electrical and optical excitation on the conductive characteristics of ITO/TiO_2/ITO structure. The conductance relaxation behaviors are observed after electrical forming and in the dark, respectively. Under the optical illumination, the conductance change of the RS device is about two orders of magnitude larger than that of the device in the pristine resistive state (PRS), but 2–3 orders of magnitude smaller than the conductance change corresponding to the variation of the background current, which manifests the emergence of a great number of oxygen vacancies in the RS device. With the illumination extinguished, the conductance decays slowly which can be ascribed to the dominant oxygen diffusion process in the conductance relaxation. The differences in conductance relaxation between the edge and bulk device suggest that the oxygen exchange through the TiO_2 edges plays a critical role in the oxygen diffusion process.

*Project supported by the National Key Basic Research Project of China (Grant Nos. 2013CB921700 and 2016YFA0300600), the National Natural Science Foundation of China (Grant No. 11274375), and the Fund from Chinese Academy of Sciences (Grant No. KJCX2-YW-W24).

†Corresponding author. E-mail: maoqi2012@gmail.com
‡Corresponding author. E-mail: hwzhao@iphy.ac.cn

© 2017 Chinese Physical Society and IOP Publishing Ltd

2. Experimental details

The ITO/TiO_2/ITO/Au films were prepared on glass substrates in a radio-frequency magnetron sputtering system.[21] The bottom ITO electrode of 400 nm in thickness was annealed at 340 °C for 10 min under an O_2 pressure of 0.2 Pa to achieve better transparency. The TiO_2 layer of 100 nm in thickness was prepared at room temperature, consequently resulting in the formation of an amorphous structure with a bandgap of about 3.45 eV.[22] The top ITO(70 nm) /Au(100 nm) electrodes were then sputtered and patterned by the standard lithography (bulk device A as shown in Fig. 1(a)). The electrode pad size was 100 μm×100 μm, the distance between two pads was about 2 mm, and a set of 8×8 top electrodes were fabricated on each substrate. In order to investigate the influence of the ambient oxygen on the RS, an etch step was introduced to remove the TiO_2 layer surrounding the top electrode, thereafter forming a TiO_2 edge underneath the top electrode (edge device B as shown in Fig. 1(a)). In this case, device B with exposed TiO_2 sidewall was prepared under the same conditions as those in the case of device A. The electrical measurements were performed with a Keithley 6430 source meter at room temperature, and the bottom ITO electrode was grounded. A xenon lamp-monochromator system was employed as a light source to illuminate the device from the glass substrate side with a focused beam spot size of about 300 μm × 800 μm and an intensity of about 1 mW/cm^2. The wavelength of the illumination light of 400 nm was chosen in order to photoionize the oxygen vacancies of the TiO_2 layers without triggering its intrinsic excitation and to stay away from the absorption edge of the glass.[22,23]

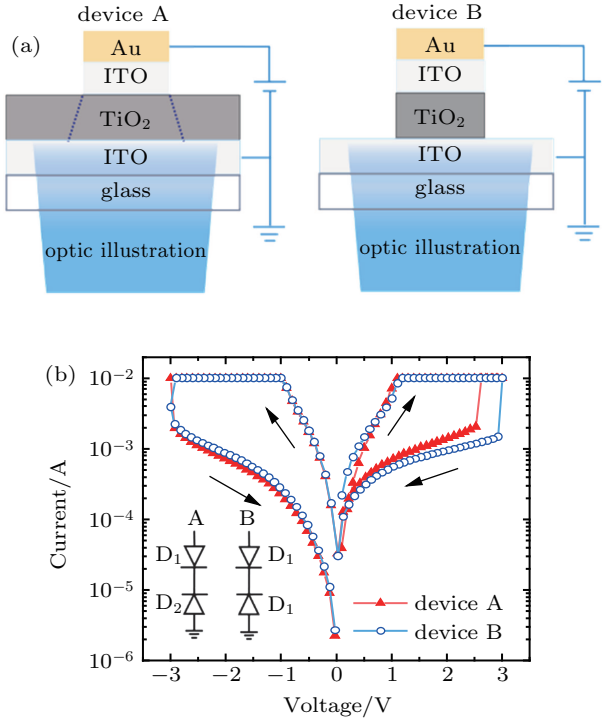


Fig. 1. (color online) (a) Schematics of ITO/TiO_2/ITO/Au devices A and B. (b) *I*–*V* curves for devices A (solid triangle) and B (solid circle), respectively, where inset shows the equivalent circuit consisting of two back-to-back diodes in series.

3. Results and discussion

First, a direct current (DC) voltage sweep of ±3.5 V is used to complete the electroforming process. After forming devices A and B show reversible RS behaviors (Fig. 1(b)). The RSs with almost symmetric nonlinear *I*–*V* curves have been reported in Pt/TiO_2/Pt layers,[24,25] and ascribed to the changes of two Schottky-like back-to-back interfacial barriers due to the drift of oxygen vacancies under an electric field. In our experiment, devices A and B exhibit almost identical *I*–*V* characteristics in the negative voltage region. In the positive branch, the switching voltage (V_{th}) of device B from the LRS to the HRS is about 3 V, larger than that of device A (2.5 V). Hence, the dissimilarity of V_{th} between devices A and B in the positive branch derives from the structural difference of the bottom Schottky barrier. More specifically, the larger value of V_{th} of device B may originate from the extra contribution of the TiO_2 edges,[26,27] as well as the ambient oxygen concentration incorporated from edge into the bulk of TiO_2.

To investigate the influence of optical illumination on the RS, the conductivity characteristics of the RS devices in the dark are firstly measured. Special care is taken to perform all electrical measurements in the dark after device preparation. After forming, the device is immediately reset/set into the HRS/LRS and the retention characteristics are measured by using a series of low read-voltages of 0.5 V (duration = 70 ms, period = 10 s) to minimize disturbance on device conductance. As shown in Fig. 2(a), the HRS conductances of devices A and B first increase rapidly ($t < 3000$ s), followed by a slow decay to reach a quasi-equilibrium state ($t > 3000$ s). In contrast, the LRS conductance decreases rapidly, then decays slowly. Similar conductivity relaxation behaviors of the RS devices have been reported previously,[8,28–30] although it has not been specified whether the measurements were performed in the dark. Nian *et al.* have analyzed the conductivity relaxation in perovskite oxide film, and proposed an oxygen diffusion model with oxygen vacancy accumulating in the electrode interface region.[8] Zhang *et al.* have observed the temperature-dependent relaxation and discussed the results in terms of the trapping/detrapping process.[31] Schulman *et al.* have ascribed the relaxation for the HRS/LRS of oxides to the diffusion of oxygen vacancies with a temperature-dependent density of trapping centers.[28] In general, the conductivity of oxide varies with oxygen concentration by surface exchange or bulk diffusion.[32,33] Accordingly, the oxygen diffusion process can be described by a single exponential function. On the other side, the thermally activated electron trapping/detrapping process at oxygen vacancies also gives rise to

conductivity relaxation, which can be phenomenologically described by a stretched exponential function.[34,35] Therefore, the overall conductivity relaxation of the RS device can be described by

$$\Delta I(t) = I_1 \exp[-(t/\tau_1)^{\beta}] + I_2 \exp(-(t/\tau_2), \qquad (1)$$

where the first term and second term correspond to the trapping/detrapping and diffusion terms, τ_1 and τ_2 are the relaxation times, and β $(0 < \beta < 1)$ is the dispersion parameter. Larger β means a narrower distribution of time constants around τ_1. In the regime of rapid variation ($t < 3000$ s), the experimental results of Fig. 2(a) can be well fitted with Eq. (1) as shown in Figs. 2(b) and 2(c). For device A in the HRS, the values of $\beta = 0.87$ and $\tau_1 = 466$ s can be extracted while in the LRS the values of $\beta = 1$ and $\tau_1 = 4382$ s are obtained. We further discuss the possible conductance change caused by different relaxation mechanisms. The oxygen vacancy diffusion of a device in the LRS should reduce the conductance, since the LRS is obtained by the drift of oxygen vacancies under an electric field. The trapping process of electrons from the conduction band to the defect level should reduce the conductance, whereas the detrapping process of electrons from the defect level to the conduction band should increase the conductance. Thus during the HRS relaxation the decrease of current would suggest that the process of thermal detrapping of electrons dominates. Similarly, during the LRS relaxation the increase of current together with $\beta = 1$ would suggest that oxygen vacancy diffusion dominates. For device B, similar curve fitting results are obtained as shown in Fig. 2(c). It is noted that the values of $\tau_1 = 466$ s and $\tau_2 = 4382$ s for device A are much larger than $\tau_1 = 307$ s and $\tau_2 = 1432$ s for device B. The fast relaxation behaviors in device B can be ascribed to more oxygen incorporated into the device from the TiO_2 edge surrounding the top electrode. Comparing the conductance relaxation of device A with that of device B, we conclude that the fast relaxations of the HRS and LRS mainly result from the thermal detrapping of electrons from oxygen vacancies and the oxygen diffusion process, respectively. Both relaxations are influenced by the oxygen exchange between devices and an ambient environment. In the regime of slow decay ($t > 3000$ s), the HRS conductance decreases with time very slowly, in contrast to the earlier sharp increase ($t < 3000$ s). The trend change of conductance from increase to decrease indicates that the oxygen transport process starts to displace the process of thermal detrapping of electrons, dominating the slow relaxation of the HRS conductance. For the slow decay of the LRS ($t > 3000$ s), the relaxation of devices A and B begins to deviate from the fitting results, where the fitted curve of device B deviates more than that of device A, which should also be ascribed to more oxygen atoms incorporated from the edge. Therefore, the slow conductance relaxations ($t > 3000$ s) of both HRS and LRS originate from the oxygen diffusion process, and their main difference is that the oxygen vacancy concentration of the HRS is less than that of the LRS, which leads to the slight difference in relaxation rate as $t > 3000$ s. However, the rate of conductance decrease is so slow that the relaxation can be approximately treated as a linear variation with time, which leads to the fact that a fitting of Eq. (1) is not applicable.

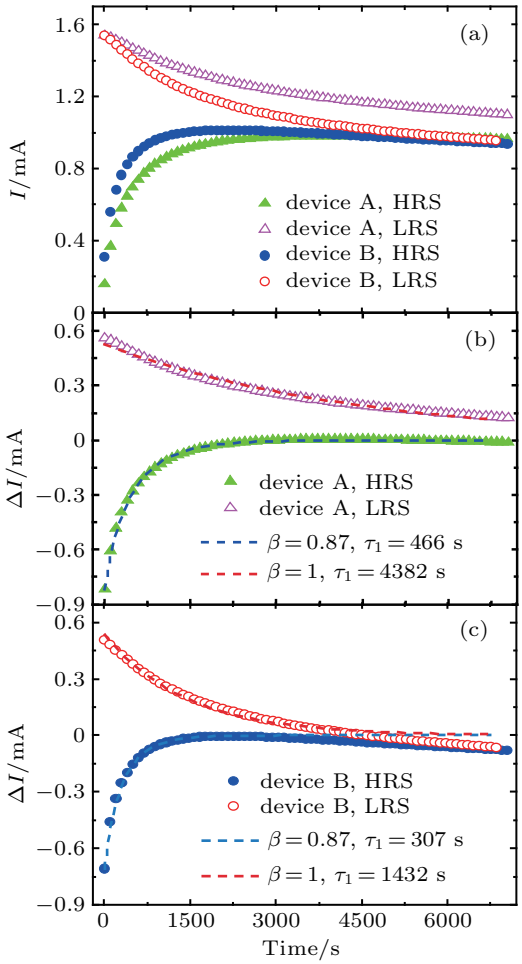


Fig. 2. (color online) (a) Current relaxations for the HRS (solid) and LRS (open) of devices A (triangle) and B (circle) in the dark. (b) and (c) Relaxation curves of devices A (triangle) and B (circle) in the HRS (solid) and LRS (open) as well as fittings (dashed lines), respectively. The bias is −0.5 V and time interval is 10 s.

Since the TiO_2 layers exhibit dark conductivity relaxation after the electrical stimulus (forming), it is necessary to investigate the conductivity characteristics of the devices in the PRS in response to optical illumination alone. By using the same voltage pulses used in Fig. 2, the conductivity characteristics of devices in the PRS are measured. Figure 3(a) shows that the dark conductances of devices A and B in the PRS are both below 1 nA and remain constant over time. Then the photoconductance is measured under optical illumination for about 500 s, followed by 2000 s in the dark. Upon illumination, the photocurrents of devices A and B increase quickly up to 13.7 nA and 8.1 nA, respectively. When the illumination is turned off ($t = t_0$), the conductance falls rapidly at first,

then decreases gradually and does not return to the previous level in the investigated time range. The dark current of the PRS is about 0.2 nA, about 5–6 orders of magnitude smaller than that of the HRS/LRS due to the generation of abundant oxygen vacancies in the RS devices after forming. Under illumination, electron-hole pairs are generated through oxygen vacancy states within the bandgap of TiO_2,[36,37] which leads to the enhanced photoconductance. After illumination, the decrease of photocurrent I_{ph} originates from two kinds of electron-consuming processes: (i) electrons are retrieved by the adsorbed oxygen, which can be described by a single exponential function;[38] (ii) electrons are trapped by oxygen vacancies with a distribution of activation energy, which can be described by a stretched exponential function.[13,34] Hence, the total photoconductance relaxation starting from t_0 can be described by an equation similar to Eq. (1):

$$I_{ph}(t) = I_1 \exp\left(\frac{-t}{\tau_1}\right) + I_2 \exp\left[-\left(\frac{t}{\tau_2}\right)^{\beta}\right], \qquad (2)$$

where τ_1 and τ_2 refer to the time constants and β is a dispersive parameter. The normalized photoconductance decay curves ($I_{ph}(t)/I_{ph}(t_0)$) are fitted with Eq. (2). The values of β and τ before and after 200 s are shown in Fig. 3(b) accordingly, which corresponds respectively to the fast and long stages observed in previous studies on ZnO.[39–41] The fast relaxation of photoconductivity decays as a single exponential function ($\beta \sim 1$), indicating that the reaction between the adsorbed oxygen and electrons in the interface region is uniform, which is consistent with the homogeneous interfacial resistive switching in amorphous oxide film. The adsorption of oxygen would increase the interfacial barrier for electrons and prevent further oxygen from being adsorbed, thus leading to the fact that the fast relaxation only dominates a short period (200 s). Therefore, for the long time relaxation of photoconductivity ($\beta \sim 0.4$), the photocurrent decay mainly originates from the electron trapping process on oxygen vacancy sites. The time constant τ of device A is always larger than that of device B, revealing that more oxygen is incorporated into TiO_2 from the exposed sidewall of device B, which leads to a faster photoconductance relaxation. Based on these results, it is clearly demonstrated that TiO_2 layers exhibit conductivity relaxation driven independently by the electrical and optical stimuli. During the relaxation, both the electron trapping/detrapping and the oxygen transport processes are involved.

Eventually, the photoconductances of the RS devices are investigated under optical illumination. Because the dark conductivity relaxation of the HRS/LRS is always present as background (Fig. 2), the total measurement time decreases to minimize the influence of background relaxation. After the RS devices are reset/set into the HRS/LRS, they are kept in the dark for about 1 h to achieve the quasi-equilibrium state. Then the devices are monitored periodically in the dark for 400 s and under illumination for 100 s to measure the conductivity characteristics. Figure 4 shows the photocurrent-time curves of the RS devices when the light is switched ON (100 s) and OFF (400 s). In region I, the dark current decreases slowly, which is consistent with the slow relaxation characteristics as shown in Fig. 2(a). Upon illumination (region II), the photocurrent increases sharply. The total current change due to optical illumination can be defined as $I_{ph} = I_{on} - I_{off} - \Delta I_0$, where I_{off}/I_{on} is the current ratio when light is OFF/ON, and ΔI_0 is the background current which can be properly derived from Fig. 2. Thereafter, the extracted photocurrent changes of 6.2 μA, 5.5 μA, and 5.1 μA are obtained for device A in the HRS, respectively. The photocurrent changes of both device A in the LRS and device B in the HRS/LRS can be obtained in the same way. By comparing the experimental results of RS devices in the dark and those under illumination, the following results and discussions are achieved.

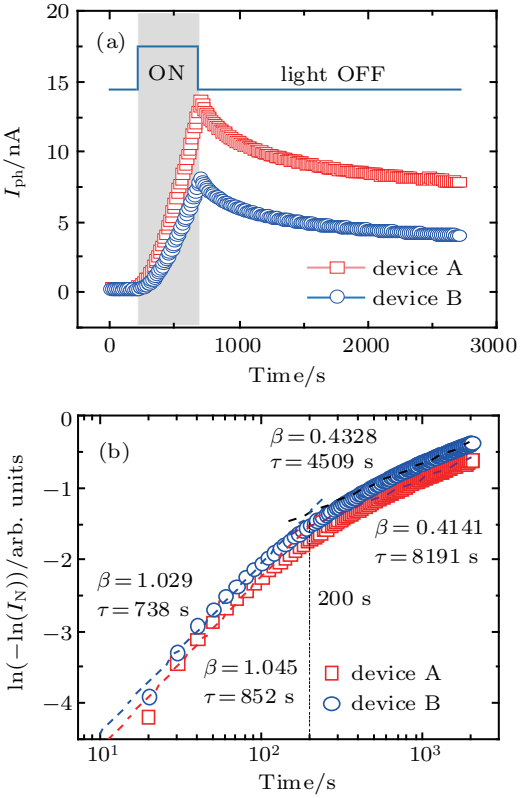


Fig. 3. (color online) (a) Time-dependent photo-excitation and dark relaxation for devices A (square) and device B (circle). (b) Stretched exponential fittings of the normalized photoconductance decay curves $I_N = I_{ph}(t)/I_{ph}(t_0)$ for devices A (solid line) and device B (dash line). The bias is −0.5 V and the time interval is 10 s.

1) Upon illumination, the photocurrent change of device A in the HRS is 6.2 μA, about two orders of magnitude larger than 13.7 nA in the PRS of device A (Fig. 3(a)). The giant enhancement of photocurrent can be ascribed to the emergence of a great number of oxygen vacancies in the RS devices after forming, which can enhance the electron–hole pairs and thermally detrap electrons. Similar behaviors are also found for

device A in the LRS (Fig. 4(c)). By contrast, the photocurrent change for device B in the HRS/LRS is much smaller than that of device A as shown in Figs. 4(b) and 4(d). The relatively fast decay of dark conductance of device B in the LRS after $t = 3000$ s can account for the behaviors (Fig. 2(a)). For device B, more oxygen absorption/exchange reactions occur at the device sidewall, which leads to a lower concentration of oxygen vacancies and correspondingly a smaller photocurrent.

The photoconductivity of the ZnO resistive device in the HRS/PRS is observed and explained by oxygen photodesorption.[17] No photocurrent is observed in the LRS because the surface depletion layer is short-cutted by the filament. Similar results have been reported in metal/Al_2O_3/SiO_2/Si and ITO/CeO_{2-x}/AlO_y/Al structures.[15,18] These devices exhibit a persistent photoconductance effect under illumination, which could change the resistance state. The persistent photoconductance could either come from the photoionization of oxygen vacancies at the interface, or from the intrinsic excitation of substrates.

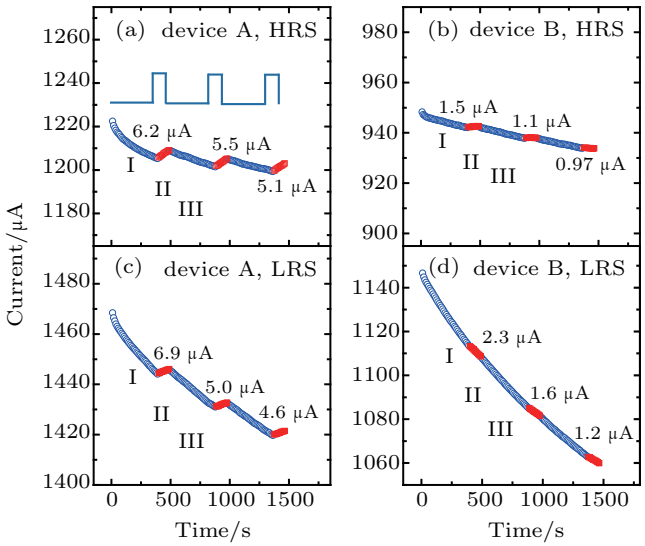


Fig. 4. (color online) Photoconductive responses of devices A and B in the HRS/LRS for periodic cycles of optical illumination. The bias is −0.5 V and time interval is 10 s.

2) With the illumination extinguished, both the photocurrent relaxation as depicted in Fig. 3 and background relaxation as investigated in Fig. 2 contribute to the overall conductance decay in region III. For the RS devices A and B in the HRS/LRS, the photocurrent change (< 10 μA) is usually 2–3 orders of magnitude smaller than the background current (~ 1000 μA) as shown in Fig. 4. The great difference in conductance indicates that the conductance decay in region III mainly comes from the background relaxation, or in other words, the oxygen diffusion process plays a decisive role in the conductance relaxations of devices A and B in the HRS/LRS with the illumination being off. However, the slow relaxation of conductance in region III is not suitable to be fitted accurately in terms of the oxygen diffusion model. This is due to the fact that the conductance variation is so slow that it can be approximately treated as a linear variation with time.

3) These results above clearly show that the RS devices exhibit conductance relaxation driven separately by the electrical and optical stimuli. However, under the joint stimuli, the conductance relaxation characteristics of RS devices are indistinguishable to some degree. Therefore, an appropriate control of the relative intensity between optical and electrical stimuli will significantly help explore the influence of optical modulation on RS devices, which has usually been ignored in previous studies.

4. Conclusions

In this work, we study the conductance characteristics of ITO/TiO_2/ITO RS devices under electrical and optical excitations. The conductivity relaxation behaviors are observed for the TiO_2 layers driven by electrical and optical stimuli separately, which can be ascribed to the thermal detrapping of electrons and the oxygen transport process. For the RS devices, the conductance change under optical illumination is much smaller than the background current due to the enhanced emergence of a great number of oxygen vacancies. With the illumination being off, the conductance decays slowly, which suggests that the oxygen diffusion process dominates the conductance relaxation. The difference in conductance relaxation between the edge and bulk devices indicates that the oxygen exchange through the TiO_2 edges plays a critical role in the relaxation process of conductivity. The unique conductance characteristics of the RS devices driven by both electrical and optical excitations could be exploited for novel applications in integrated optoelectronic memory devices.

References

[1] Dearnaley G, Stoneham A M and Morgan D V 1970 *Rep. Prog. Phys.* **33** 1129
[2] Rozenberg M J, Inoue I H and Sánchez M J 2004 *Phys. Rev. Lett.* **92** 178302
[3] Waser R and Aono M 2007 *Nat. Mater.* **6** 833
[4] Waser R, Dittmann R, Staikov G and Szot K 2009 *Adv. Mater.* **21** 2632
[5] Yang J J, Miao F, Pickett M D, Ohlberg D A A, Stewart D R, Lau C N and Williams R S 2009 *Nanotechnology* **20** 215201
[6] Bae Y C, Lee A R, Kwak J S, Im H, Do Y H and Hong J P 2011 *Appl. Phys. A* **102** 1009
[7] Raghavan N, Pey K Let and Liu W H, Wu X, L X and Bosman M 2011 *Microelectronic Engineering* **88** 1124
[8] Nian Y B, Strozier J, Wu N J, Chen X and Ignatiev A 2007 *Phys. Rev. Lett.* **98** 146403
[9] Pickett M D, Strukov D B, Borghetti J L, Yang J J, Snider G S, Stewart D R and Williams R S 2009 *J. Appl. Phys.* **106** 074508
[10] Strukov D B, Snider G S, Stewart D R and Williams R S 2008 *Nature* **453** 80
[11] Golego N, Studenikin S A and Cocivera M 2000 *Phys. Rev. B* **61** 8262
[12] Zhu Q, Xie C S, Li H Y, Zhang J and Zeng D W 2015 *Chem. Mater.* **27** 2861
[13] Luo J J, Adler A U, Mason T O, Buchholz D B, Chang R P H and Grayson M 2013 *J. Appl. Phys.* **113** 153709

[14] Huo N J, Yang S X, Wei Z M and Li J B 2013 *J. Mater. Chem. C* **1** 3999
[15] Ungureanu M, Zazpe R, Golmar F, Stoliar P, Llopis R, Casanova F and Hueso L E 2012 *Adv. Mater.* **24** 2496
[16] Park J, Lee S and Yong K 2012 *Nanotechnology* **23** 385707
[17] Retamal J R D, Kang C F, Ho C H, Ke J J, Chang W Y and He J H 2014 *Appl. Phys. Lett.* **105** 253111
[18] Tan H W, Liu G, Zhu X J, Yang H L, Chen B, Chen X X, Shang J, Lu W D, Wu Y H and Li R W 2015 *Adv. Mater.* **27** 2797
[19] Borkar H, Thakre A, Kushvaha S S, Aloysius R P and Kumar A 2015 *RSC Adv.* **5** 35046
[20] Wei L, Li G Q and Zhang W F 2016 *J. Phys. D: Appl. Phys.* **49** 045101
[21] Meng Y, Zhang P J, Liu Z Y, Liao Z L, Pan X Y, Liang X J, Zhao H W and Chen D M 2010 *Chin. Phys. B* **19** 037304
[22] Takeuchi M 1979 *Phys. Stat. Sol. (a)* **55** 653
[23] Bansal N P and Doremus R H 1986 *Handbook of Glass Properties* (New York: Academic Press) p. 44
[24] Jeong D S, Schroeder H and Waser R 2009 *Phys. Rev. B* **79** 195317
[25] Yang J J, Pickett M D, Li X M, Ohlberg D A A, Stewart D R, Lau C N and Williams R S 2008 *Nat. Nanotechnol.* **3** 429
[26] Chang Y F, Ji L, Wang Y Z, Chen P Y, Zhou F, Xue F, Fowler B, Yu E T and Lee J C 2013 *Appl. Phys. Lett.* **103** 193508
[27] Fowler B W, Chang Y F, Zhou Fei, Wang Y Z, Chen P Y, Xue F, Chen Y T, Bringhurst B, Pozder S and Lee J C 2015 *RSC Adv.* **5** 21215
[28] Schulman A, Rozenberg M J and Acha C 2012 *Phys. Rev. B* **86** 104426
[29] Chang T, Jo S H and Lu W 2011 *ACS Nano* **5** 7669
[30] Das N, Tsui S, Xue Y Y, Wang Y Q and Chu C W 2009 *Phys. Rev. B* **80** 115411
[31] Zhang H J, Zhang X P, Zhao Y G 2009 *Chin. Phys. Lett.* **26** 077303
[32] Bieger T, Maier J and Waser R 1992 *Sensors and Actuators B: Chemical* **7** 763
[33] Merkle R and Maier J 2008 *Angew. Chem. Int. Ed.* **47** 3874
[34] Redfield and Bube R H 1996 *Photo-induced Defects in Semiconductors* (New York: Cambridge University Press) p. 66
[35] Kim J Y, Yu K M, Jeong S H, Yun E J and Bae B S 2014 *Can. J. Phys.* **92** 611
[36] Moazzami K, Murphy T E, Phillips J D, Cheung M C K and Cartwright A N 2006 *Semicond. Sci. Technol.* **21** 717
[37] Yang C Q, Zhu Q, Zhang S P, Zou Z J, Tian K and Xie C S 2014 *Appl. Surf. Sci.* **297** 116
[38] Sakaguchik, Shimakawak K and Hatanaka Y 2006 *Jpn. J. Appl. Phys.* **45** 4183
[39] Wu T H, Cheng I C, Hsu C C and Chen J Z 2015 *J. Alloys Compd.* **628** 68
[40] Sharma P, Sreenivas K and Rao K V 2003 *J. Appl. Phys.* **93** 3963
[41] Ahn S E, Lee J S, Kim H, Kim S, Kang B H, Kim K H and Kim G T 2004 *Appl. Phys. Lett.* **84** 5022